Molecular Genetics and Metabolism 94 (2008) 298–304

Contents lists available at ScienceDirect

Molecular Genetics and Metabolism

journal homepage: www.elsevier.com/locate/ymgme

Upregulation of elastase proteins results in aortic dilatation in mucopolysaccharidosis I mice

Xiucui Ma [a], Mindy Tittiger [a], Russell H. Knutsen [b], Attila Kovacs [a], Laura Schaller [a,b,c], Robert P. Mecham [b], Katherine P. Ponder [a,c,*]

[a] Department of Internal Medicine, Washington University School of Medicine, 660 South Euclid Avenue, St. Louis, MO 63110, USA
[b] Department of Cell Biology, Washington University School of Medicine, St. Louis, MO, USA
[c] Department of Biochemistry and Molecular Biophysics, Washington University School of Medicine, St. Louis, MO, USA

ARTICLE INFO

Article history:
Received 27 February 2008
Received in revised form 26 March 2008
Accepted 27 March 2008
Available online 13 May 2008

Keywords:
Hurler syndrome
Lysosomal storage disease
Elastin
Aorta
Gene therapy

ABSTRACT

Mucopolysaccharidosis I (MPS I), known as Hurler syndrome in the severe form, is a lysosomal storage disease due to α-L-iduronidase (IDUA) deficiency. It results in fragmentation of elastin fibers in the aorta and heart valves via mechanisms that are unclear, but may result from the accumulation of the glycosaminoglycans heparan and dermatan sulfate. Elastin fragmentation causes aortic dilatation and valvular insufficiency, which can result in cardiovascular disease. The pathophysiology of aortic disease was evaluated in MPS I mice. MPS I mice have normal elastic fiber structure and aortic compliance at early ages, which suggests that elastin assembly is normal. Elastin fragmentation and aortic dilatation are severe at 6 months, which is temporally associated with marked increases in mRNA and enzyme activity for two elastin-degrading proteins, matrix metalloproteinase-12 (MMP-12) and cathepsin S. Upregulation of these genes likely involves activation of STAT proteins, which may be induced by structural stress to smooth muscle cells from accumulation of glycosaminoglycans in lysosomes. Neonatal intravenous injection of a retroviral vector normalized MMP-12 and cathepsin S mRNA levels and prevented aortic disease. We conclude that aortic dilatation in MPS I mice is likely due to degradation of elastin by MMP-12 and/or cathepsin S. This aspect of disease might be ameliorated by inhibition of the signal transduction pathways that upregulate expression of elastase proteins, or by inhibition of elastase activity. This could result in a treatment for patients with MPS I, and might reduce aortic aneurism formation in other disorders.

Introduction

Mucopolysaccharidosis I (MPS I) is an autosomal recessive lysosomal storage disease due to α-L-iduronidase (IDUA; EC 3.2.1.76) deficiency that results in the accumulation of the glycosaminoglycans (GAG) heparan and dermatan sulfate [1]. The severe (Hurler syndrome), intermediate (Hurler–Scheie syndrome), and mild (Scheie syndrome) forms of MPS I can all result in fragmented elastin fibers in the ascending aorta and cardiac valves in humans [2,3], which can result in aortic insufficiency due to reduced structural integrity of the valve. Dog [4,5] and mouse [3,6,7] models of MPS I also have elastin fragmentation of the ascending aorta and heart valves, which can result in aortic dilatation in addition to aortic insufficiency.

Elastic fibers are complex structures that consist primarily of tropoelastin monomers organized into a highly crosslinked polymer in a process that involves elastin binding protein (EBP), components of extracellular matrix microfibrils, and crosslinking enzymes [8]. Abnormalities in any of the molecules or assembly steps could result in the fragmented elastic fibers seen in MPS I tissues. Indeed, EBP levels were low and elastin biogenesis was reduced in fibroblasts from patients with MPS I, and it was proposed that defects in elastin assembly resulted in fragmented elastic fibers in the aorta [9].

An alternative explanation for elastin fragmentation is that MPS I results in activation of elastin-degrading proteins such as metalloproteinases (MMPs), cathepsins, or neutrophil elastase [10,11]. The metal-dependent MMP-2, 7, 8, 9, 10, 12, and 14 can degrade elastin and/or play a role in aortic aneurisms [12–15]. Furthermore, MMP-9 or MMP-12 deficiency reduced elastin fragmentation within atherosclerotic lesions in hypercholesterolemic mice [14] or reduced $CaCl_2$-induced aneurism formation [12,16]. In addition, deficiency of MMP-9, but not MMP-12, reduced aneurism formation after elastase perfusion [13]. MMPs are activated proteolytically by urokinase plasminogen activator (uPA), or without cleavage by SIBLINGs (small integrin-binding ligand N-linked glycoproteins) such as osteopontin [17]. uPA deficiency reduced aneu-

* Corresponding author. Address: Department of Internal Medicine, Washington University School of Medicine, 660 South Euclid Avenue, St. Louis, MO 63110, USA. Fax: +1 314 362 8813.
E-mail address: kponder@im.wustl.edu (K.P. Ponder).

1096-7192/$ - see front matter © 2008 Elsevier Inc. All rights reserved.
doi:10.1016/j.ymgme.2008.03.018

rism formation [10] while osteopontin is upregulated in aortic aneurisms [15]. Tissue inhibitor of metalloproteinases (TIMP) 1 binds and inactivates MMPs, while TIMP-2 protects MMPs from inactivation by TIMP-1; TIMP-1 overexpression [18] and TIMP-2 [19] deficiency reduced aneurism formation in mice.

Cathepsins are lysosomal cysteine proteases that can degrade elastin and are upregulated in aneurisms [11]. Although most are rapidly inactivated at the neutral pH found in the extracellular space, cathepsin S maintains 64% of its peak activity at pH 7.5 [20]. Cathepsin S RNA is increased in atherosclerotic lesions in mice [21] and its deficiency reduced elastin fiber fragmentation in hypercholesterolemic mice [22]. Cystatin C is a cathepsin inhibitor, and its mRNA is reduced in human aortic aneurisms, and its deficiency increases elastin fragmentation in hypercholesterolemic mice [11].

The goal of this study was to determine the pathogenesis of elastic fiber fragmentation in the ascending aorta of MPS I mice. We demonstrate here that elastin structure and function are normal in young mice, suggesting that MPS I does not adversely affect elastin synthesis and assembly *in vivo*. However, increases in mRNA and enzyme activity for the elastolytic proteases MMP-12 and cathepsin S correlated with progressive elastin fragmentation and aortic dilatation in older mice, suggesting that the mechanism underlying aortic disease in MPS I is enhanced elastin degradation.

Materials and methods

Reagents were from Sigma-Aldrich Chemical (St. Louis, MO) unless otherwise stated.

Animals

Animal studies were approved by our Institutional Review Board. MPS I mice [23] were on a C57BL/6 background and normal controls were heterozygous littermates. Some MPS I mice were injected IV with 10^{10} transducing unit (U) U/kg of the retroviral vector hAAT-cIDUA-WPRE at 2–3 days after birth [7]. For compliance curves, periadventitial fat was removed from ascending aortas and the outer diameters determined halfway between the sinotubular junction and the innominate artery [23]. Echocardiography was performed with a Vevo 770 echocardiography machine (VisualSonics, Toronto ON) using inhaled isofluorane anaesthesia.

Pathology

Ascending aortas were fixed as described [7] and a region 3 mm from the aortic valve was obtained. Six micrometer sections were stained with Verhoeff's Van Gieson (VVG) stain. A micrometer was used to measure a length of 0.4 mm that was parallel to the elastic fibers, and the number of fragmented elastin fibers throughout all layers of the aorta was determined at >5 different regions. The number of breaks per millimeter aorta length was calculated.

RNA analysis

For RNA and enzyme analysis, the ascending aorta from the sinotubular junction to the innominate artery was stripped of periadventitial tissue. A 5–10 mg piece was homogenized for 30 s in 150 μl of RNeasy micro kit buffer (Qiagen Inc., Valencia, CA) with a hand-held pellet pestle (Kimble-Kontes; Vineland, NJ) and incubated for 10 min with proteinase K and purified according to the manufacturer's instructions. Reverse transcription (RT) was performed on DNase I-treated RNA with an oligo (dT) 20 primer using a Superscript III kit from Invitrogen Corp. (Carlsbad, CA) in a 20 μl volume, followed by real-time PCR on 0.4 μl of each cDNA sample per well using SYBR green reagents from Applied Biosystems (Foster City, CA) unless otherwise stated. The primers are listed in Table 1 of the supplementary methods section. The percent of an RNA to that of β-actin was calculated by subtracting the cycle to reach the threshold (C_T) for a gene from the β-actin C_T to determine the ΔC_T, and the formula: Percent β-actin = ð100Þ $2^{\Delta C_T}$.

MMP-12 and cathepsin S activity assays

An MMP-12 assay kit (EnzolyteTM 490 MMP-12) was obtained from Anaspec (San Jose, CA). According to the manufacturer, the substrate is also cleaved by MMP-1, 2, 3, 8, and 13. Ascending aortas were homogenized in 100 μl of assay buffer, centrifuged at 10,000*g* for 5 min at 4 °C, and the protein concentration determined with the Bradford assay (Bio-Rad Laboratories, Hercules CA). Approximately 3 μg of extract was assayed in a 100 μl volume using substrate concentrations recommended by the manufacturer, and the fluorescent units were measured every 5 min with a Fluoroskan Ascent microplate fluorometer from Thermo Electron Corporation (Milford, MA) with excitation at 355 nm and emission at 460 nm. Standards were 5-[(2-aminoethyl)amino]naphthalene-1-sulfonic acid in assay buffer. One unit of enzyme releases 1 nmol of product per hour at 37 °C. All inhibitors were from Calbiochem (San Diego CA) and were used at the following final concentration. EDTA (10 mM) and EGTA (10 mM) chelate metals; cathepsin inhibitor I (Z-Phe-Gly-NHO-Bz; 200 μM) inhibits cathepsins B, L, and S; cathepsin S inhibitor Z-FL-COCHO (10–1000 pM) inhibits cathepsin S; calpain inhibitor I (20 μg/ml) inhibits cathepsin B and L and calpain I and II; the sulfhydryl inhibitor iodoacetamide inhibits cathepsins and other cysteine proteases; phenylmethylsulfonyl fluoride (PMSF; 1 mM) inhibits serine proteases; pepstatin A (1 μM) inhibits cathepsin D, pepsin, and renin; and bestatin (10 μM) inhibits aminopeptidase B and leucine aminopeptidase. Samples were incubated with the inhibitor for 10 min at 4 °C prior to starting the assay.

For the cathepsin S assay, aortas were homogenized in 100 mM Na–Acetate pH 5.5 containing 2.5 mM EDTA, 0.01% Triton X-100, and 2.5 mM dithiothreitol (DTT). Assays used 20 μM benzyloxycarbonyl-L-phenylalanyl-L-arginine-7-amido-4-methylcoumarin (Z-Phe-Arg-AMC; Anaspec) at pH 7.5 in 100 mM Na–Acetate with 2.5 mM EDTA, 0.01% Triton X-100, and 2.5 mM DTT in a microtiter plate [24] with 0.3 μg of extract at 37 °C. The amount of product was determined by excitation at 355 nm and emission at 460 nm using a kinetic reading for a microtiter plate and comparison with 7-amino-4-methylcoumarin standards from Anaspec. One unit of enzyme releases 1 nmol of the product per hour at 37 °C.

Immunohistochemistry

Aortas were embedded in OCT from Akura Finetek (Torrance, CA) and 8 μm-thick sections were mounted on Superfrost adhesive slides (Fisher Scientific, USA) and fixed with 4% paraformaldehyde in PBS for 20 min at 4 °C. Endogenous peroxidase activity was inhibited using 0.6% hydrogen peroxidase in Tris Buffered Saline (TBS; 40 mM Tris pH 7.4 with 150 mM NaCl). Staining was performed using polyclonal rabbit antibodies from Cell Signaling Technology (Danvers MA) that were diluted 1:100. After overnight incubation at 4 °C with the first antibody in blocking buffer (TBS with 10% normal goat serum), samples were incubated with a 1:200 dilution of biotinylated anti-rabbit antibody (VECTOR Laboratories, Inc., Burlingame CA) for 1 h at room temperature, and developed with the ABC reagents provided in the kit. Negative controls used non-specific rabbit IgG as the primary antibody.

Statistics

The Student's *t* test compared values between 2 groups, and ANOVA with Tukey post hoc analysis compared values between 3 groups using Sigma Stat software (Systat Software, Inc., Point Richmond, CA).

Results

Effect of age and gene therapy on aorta dilatation and elastin fragmentation

The time course of development of ascending aortic dilatation and elastin fragmentation in MPS I mice was evaluated by studying the mechanical properties and pathology of aortas at different ages at a point halfway between the sinotubular junction and the innominate artery (Fig. 1). The outer diameters of ascending aortas from MPS I mice were modestly dilated at 1.5 and 3 months when 75 mm of Hg of pressure was applied at 1.6 ± 0.1 and 1.7 ± 0.2 mm [error bars represent standard deviation (SD)], respectively, which were statistically higher than the values of 1.4 ± 0.08 and 1.4 ± 0.03 mm in age-matched heterozygous normal littermates, respectively ($p = 0.005$ and 0.027, respectively). Aortas from MPS I mice were massively dilated at 3.3 ± 0.5 and 3.2 ± 0.6 mm at 6 and 8 months, respectively, which was >2-fold the normal value of 1.5 ± 0.05 mm in 6-month-old and 1.5 ± 0.1 in 8-month-old normal mice (A).

Echocardiography at 8 months of age demonstrated that the internal diameter at a similar region of the aorta was 2.3 ± 0.5 mm in MPS I mice, which was 1.5-fold the value of 1.6 ± 0.1 mm in normal mice (B and C; $p = 0.01$). In addition, the aorta of MPS I mice was dilated at the aortic valve (1.2-fold; 1.17 ± 0.13 mm for normal and 1.37 ± 0.06 mm for MPS I; $p = 0.01$), sinus of Valsalva (1.2-fold; 2.12 ± 0.20 mm for normal

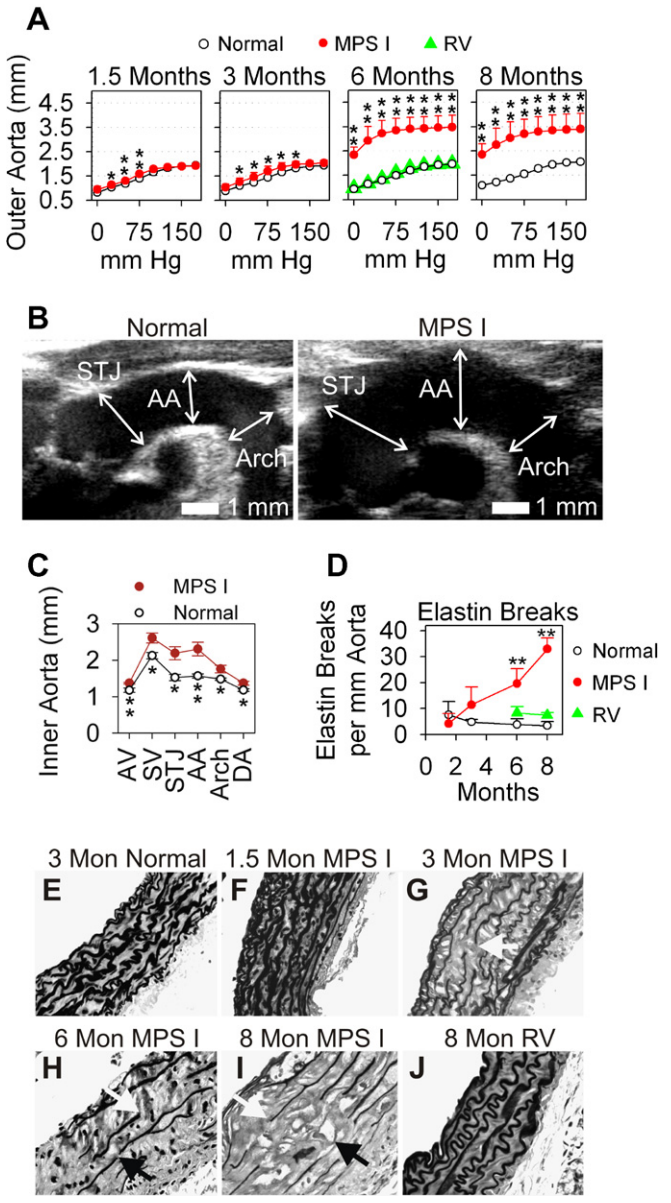

Fig. 1. Aortic diameter and elastin histochemistry. (A) Outer diameter of aortas. The average outer diameter of ascending aortas ± standard deviation (SD) at the indicated age after birth was determined at the indicated pressures for 5–6 animals in each group. Untreated MPS I and normal mice were evaluated at all times. Retroviral vector-treated MPS I mice were evaluated at 6 months and appear as the triangles that are almost indistinguishable from the values in normal mice. * indicates a p value of 0.01–0.05 and ** indicates a p value <0.01 when values in other groups were compared with those in normal mice. (B and C) Internal aortic diameter. The internal diameter of aortas from normal and untreated MPS I mice was determined by echocardiography at 8 months. (B) Representative examples of end-diastolic images, while (C) the average end-diastolic diameter for 5–7 animals in each group at the aortic valve (AV), sinus of Valsalva (SV), sinotubular junction (STJ), ascending aorta (AA), aortic arch (Arch), and descending aorta (DA). (D) Elastin breaks in the aorta. The number of elastin breaks throughout the thickness of the aorta was determined as described in Materials and methods. (E–J) Elastin stain of ascending aorta. A VVG stain for elastin was performed on an ascending aorta from a normal mouse at 3 months (E), on aortas from untreated MPS I mice at 1.5–8 months (F–I), or on an aorta from a retroviral vector (RV)-treated MPS I mouse at 8 months. The adventitia is at the bottom right, and the intima is at the top left. Fragmented elastin fibers are identified with white arrows, and lysosomal storage with black arrows.

and 2.61 ± 0.37 for MPS I; $p = 0.02$), sinotubular junction (1.4-fold; 1.50 ± 0.19 mm for normal and 2.19 ± 0.48 mm for MPS I; $p = 0.02$), arch (1.2-fold; 1.48 ± 0.07 mm for normal and 1.76 ± 0.27 mm for MPS I; $p = 0.05$), and the descending aorta (1.2-fold; 1.18 ± 0.08 mm for normal and 1.37 ± 0.14 mm for MPS I; $p = 0.02$). A video of the aortas can be viewed in the online version.

Panel D quantifies the number of elastin breaks in the ascending aorta, and E–J show representative examples of the elastin stains that were used to obtain these data. There were very few fragmented elastin fibers at early times in MPS I mice, but there were 5- and 10-fold as many elastin fiber breaks in MPS I mice as in normal mice at 6 and 8 months, respectively. Lysosomal storage material was minimal at early times and apparent at 6 and 8 months, although this was harder to appreciate on the relatively thick paraffin sections used here than in our previous study that used thin plastic sections [7].

Previously, we reported that neonatal intravenous (IV) injection of a retroviral vector expressing canine IDUA resulted in high IDUA activity in liver, serum, and aorta, and this prevented the accumulation of lysosomal storage, elastin fragmentation, and aortic dilatation in MPS I mice [7]. The mechanism of correction was probably secretion of mannose 6-phosphate (M6P)-modified IDUA by transduced hepatocytes or other cells into blood, diffusion of enzyme to the aorta, and uptake of enzyme by cells via the M6P receptor. Retroviral vector-treated MPS I mice had normal compliance curves at 6 months (Fig. 1A), and there were only 8.3 ± 2.4 and 7.5 ± 0.8 elastin fiber breaks per mm of aorta at 6 and 8 months, respectively (Fig. 1D).

mRNA levels for genes of elastin biogenesis or degradation

Genes that play a role in elastin or collagen biogenesis were expressed at normal levels in MPS I aortas at 6–8 months after birth, as determined by the real-time reverse transcriptase (RT) PCR shown in Fig. 2A. However, there were striking and statistically significant elevations in mRNA for two elastin-degrading proteins, matrix metalloprotease-12 (MMP-12; 23 ± 6-fold normal) and cathepsin S (11 ± 2-fold normal). In addition, there were elevations in mRNA for a protein that can degrade collagen but not elastin (MMP-3 at 7-fold normal), proteins that can activate MMPs (osteopontin at 16-fold normal and uPA at 3-fold normal), proteins that can associate with MMPs and affect their activity (TIMP-1 at 4-fold normal and TIMP-2 at 2-fold normal), and cathepsins that have low activity at neutral pH (cathepsin B at 2-fold normal, cathepsin D at 3-fold normal, and cathepsin L at 2-fold normal). In general, mRNA levels for genes that were elevated at 6 to 8 months were relatively normal at 1.5 months and modestly elevated at 3 months (Fig. 2B), which correlates well with the time course of lysosomal storage accumulation, elastin fiber fragmentation, and aortic dilatation. mRNA levels were normal for MMP-12 and cathepsin S in retroviral vector-treated MPS I mice at 6–8 months of age. However, osteopontin and TIMP-1 mRNA remained elevated in retroviral vector-treated mice at 7- and 3-fold normal, respectively, and values were not significantly different from those in untreated MPS I mice.

MMP-12 activity

Ascending aorta extracts were tested for MMP activity. Cleavage of a peptide that is recognized by MMP-12 was 8-fold normal in MPS I mice at 6 months ($p < 0.001$; Fig. 3A), although it is possible that some other MMP such as MMP-3 contributed to this enzyme activity, as detailed in the methods. This activity was inhibited by the metal chelators EDTA and EGTA, but was not affected by other protease inhibitors (Fig. 3B).

Cathepsin S activity

Although the substrate Z-Phe-Arg-AMC is cleaved by cathepsins B and L in addition to cathepsin S, only cathepsin S is stable at pH 7.5 [20] that was used for the reaction. Cathepsin S activity was

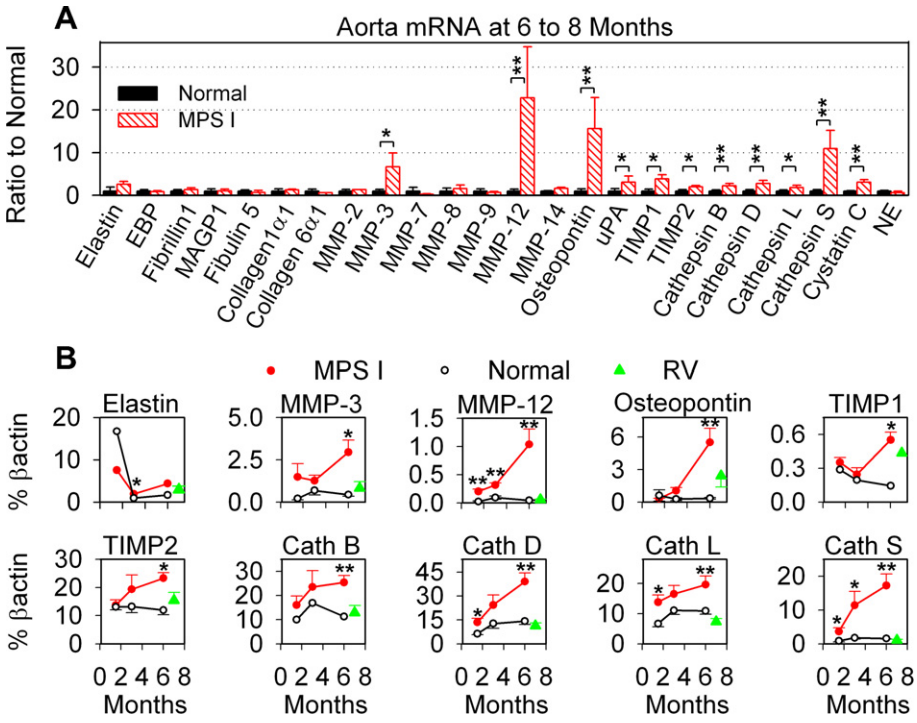

Fig. 2. mRNA levels of genes involved in extracellular matrix biogenesis and degradation. Real-time RT-PCR was used to determine the amount of each mRNA in the aorta for 3–6 mice in each group. (A) mRNA relative to normal at 6–8 months. The average ratio to normal ± SD was determined for each gene in aortas isolated at 6–8 months. Abbreviations are elastin binding protein (EBP), microfibril-associated glycoprotein (MAGP), matrix metalloproteinase (MMP), urokinase plasminogen activator (uPA), tissue inhibitor of metalloproteinase (TIMP), and neutrophil elastase (NE). (B) Time course of mRNA levels relative to β-actin. RNA from untreated MPS I and normal mice was evaluated at all times. RNA from retroviral vector (RV)-treated MPS I mice was only evaluated at 6–8 months, and the values were artifacturally plotted at a slightly later time to distinguish them from values in normal mice. The ratio of the signal for each mRNA to β-actin was determined by a comparison of the C_T values. * indicates a p value of 0.01–0.05 and ** indicates a p value <0.01 when values in other groups were compared with those in normal mice.

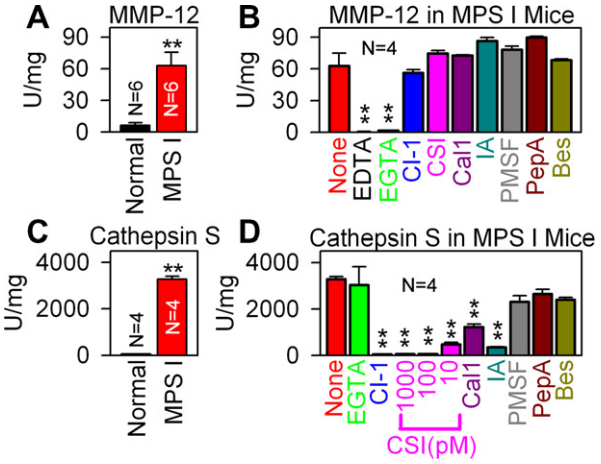

Fig. 3. Evaluation of MMP-12 and cathepsin S activity. Ascending aortas were isolated at 6–8 months after birth from untreated MPS I or normal mice. (A and B) MMP-12 activity. In (A), average MMP-12 activity ± SD was determined for 6 mice for each group, and * indicates a p value of 0.01–0.05 and ** indicates a p value <0.01 when values in MPS I mice were compared with those in normal mice. In (B), samples from MPS I mice were incubated with protease inhibitors, and activity with the inhibitor was compared with the activity without the inhibitor for samples from 4 different mice, with the same criterion for statistically significance as shown in (A). Abbreviations include cathepsin inhibitor 1 (CI-1), cathepsin S inhibitor (CSI; 1 nM was used), calpain inhibitor I (Cal1), iodoacetamide (IA), phenylmethylsulfonyl fluoride (PMSF), pepstatin A (PepA), and bestatin (Bes). (C and D) Cathepsin S activity. In (C), cathepsin S activity was determined for 4 mice from each group using Z-Phe-Arg-AMC at pH 7.5, while (D) tests the effect of inhibitors upon activity in MPS I mice.

markedly elevated at 65-fold normal ($p < 0.001$) at 6 months in MPS I mice (Fig. 3C). The response to inhibitors confirmed that this activity was due to cathepsin S, as it was inhibited with very low concentrations of a cathepsin S-specific inhibitor in addition to being inhibited by a non-specific cathepsin inhibitor and by iodoacetamide (Fig. 3D).

Mechanism for upregulation of MMP-12 and cathepsin S

The MMP-12 promoter contains binding sites for STAT-5, N-myc, CCAAT, PEA3, AP-1 (fos/jun dimers), and ets-1 [25] and sequence analysis suggests that it should also bind STAT-1 and STAT-3 [26]. Phosphorylation of STATs at tyrosine residues results in dimerization, translocation to the nucleus, DNA binding, and activation of responsive genes. In addition, the activity of STATs is increased by phosphorylation of serines by mitogen-activated protein kinase (MAPK) [26]. Immunostaining of ascending aortas isolated from MPS I mice at 8 months showed a marked increase in nuclear levels of STAT-1 that was phosphorylated at Ser727 and Tyr701, and in STAT-3 that was phosphorylated at Ser727, and Tyr705 (Fig. 4). In addition, MAPK was activated by phosphorylation at Thr202/Tyr204. In contrast, there were very low levels of STAT-5 that was phosphorylated at Tyr694 (data not shown). mRNA levels for transcription factors that are regulated transcriptionally and can influence MMP-12 expression were not altered in ascending aortas from MPS I (Fig. 5).

Although the cathepsin S promoter does not contain STAT binding sequences, it binds interferon-regulated factor 1 (IRF-1), which is regulated transcriptionally by activated STATs [27]. Indeed, although the mRNA for IRF-1 was not elevated in MPS I mouse ascending aorta (Fig. 5), mRNA for the related proteins IRF-8 and IRF-3 were 2.3 ± 0.5-fold ($p = 0.04$ *vs.* normal) and 1.6 ± 0.2-fold normal ($p = 0.02$ *vs.* normal), respectively, at 6 to 8 months. In addition, mRNA for PU.1, a transcription factor that can increase

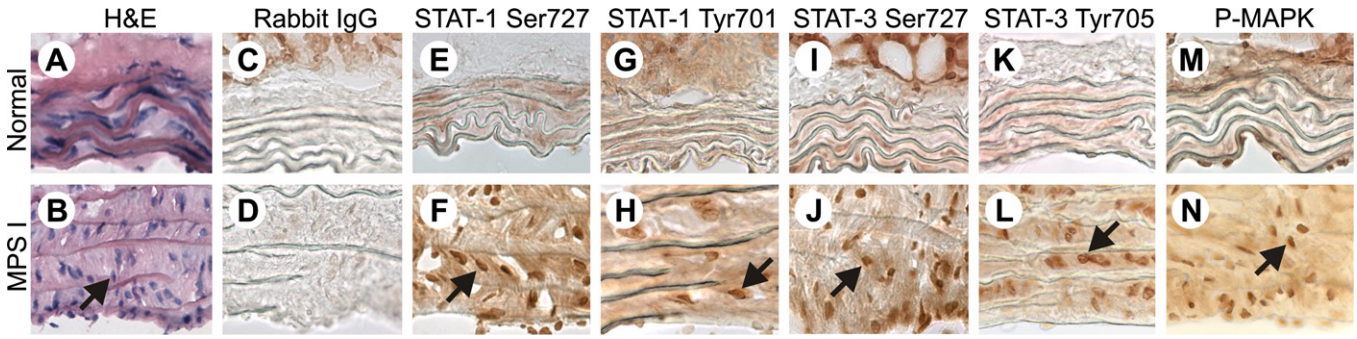

Fig. 4. Immunostaining for phosphorylated transcription factors. Ascending aortas from normal or untreated MPS I mice collected at 8 months were immunostained with antibodies specific for transcription factors that were activated by phosphorylation at the indicated amino acid. (A and B) Hematoxylin and eosin stain (H and E). The black arrows indicate smooth muscle cell nuclei (blue). (C and D) Negative control. Negative controls that received a non-specific rabbit IgG antibody as the first antibody. (E and F) STAT-1 Ser727. The black arrow indicates a nucleus with STAT-1 that is phosphorylated at serine 727, which stains brown. (G and H) STAT-1 Tyr701. (I and J) STAT-3 Ser727. (K and L) STAT-3 Tyr705. (M and N) MAPK Thr202/Tyr204.

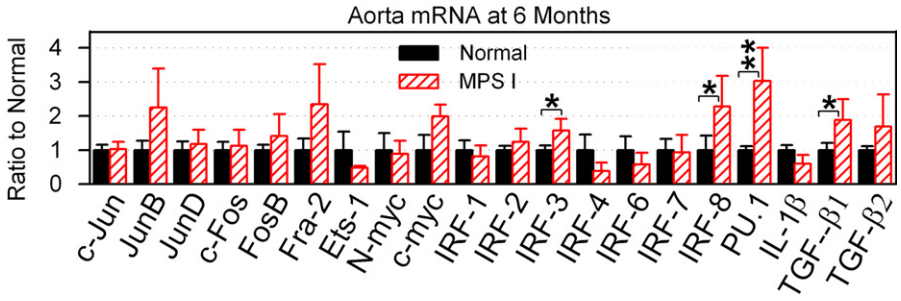

Fig. 5. Evaluation of transcription factor mRNA in aorta. Aortas obtained at 6–8 months after birth were evaluated for levels of mRNAs that are known to regulate MMP-12 or cathepsin S transcriptionally, and shown as the average relative to normal ± SD for 4–6 animals in each group. IL-1β represents interleukin 1β. * indicates a p value of 0.01–0.05 and ** indicates a p value <0.01 when values in other groups were compared with those in normal mice.

expression of cathepsin S [28] was 3.0 ± 0.5-fold normal in MPS I mice ($p = 0.01$ *vs.* normal). Activation of SMAD2 via the TGF-β receptor has been implicated in the pathophysiology of Marfan Syndrome, which is also associated with progressive fragmentation of elastin fibers [29]. Indeed, aortas from MPS I mice had a modest increase in the RNA levels of TGF-β1 to 1.9-fold normal, although there was no increase in RNA levels for TGF-β2, and there was no increase with immunostaining in the level of SMAD2 that was phosphorylated at Ser465 and Ser467 in the aorta of MPS I mice (date not shown).

Discussion

The etiology of elastin fragmentation in the aorta and heart in MPS I is important because it is a major cause of morbidity, and is relatively refractory to treatments. For example, aortic insufficiency developed *de novo* or worsened in 89% of patients at 12 years after performing hematopoietic stem cell transplantation at 2 years [30] and in 60% of patients at 4–6 years after starting enzyme replacement therapy [31,32]. Although pathological data were not available, progressive fragmentation of the elastic fibers likely contributed to worsening aortic valve function. In addition, gene therapy in mice [7] and dogs [5] only fully reduced aortic elastin fragmentation if serum IDUA activity was very high. The dense structure of the aorta likely reduces diffusion of enzyme, which may explain why the middle region is most refractory to treatment after gene therapy [5,7].

The role of MMP-12 and cathepsin S in aortic elastin fragmentation

Elastin fiber fragmentation could be due to defects in elastin assembly or to elastin degradation. Our findings of relatively normal elastic fiber structure and vessel compliance in young adult MPS I mice suggest that elastin synthesis and elastic fiber assembly are normal during the formative period of the vessel wall. This finding is in contrast to the abnormal elastic fiber assembly reported *in vitro* for fibroblasts from MPS I patients, which was associated with low EBP levels [9]. EBP is an enzymatically-inactive splice variant of β-galactosidase that binds to galactose moieties and potentiates elastin assembly [33] and it was proposed that the accumulation of the *N*-acetylgalactosamine-containing dermatan sulfate reduced EBP levels and prevented EBP from functioning as a chaperone for elastin biogenesis [9]. It remains possible that a defect in EBP-mediated elastin assembly contributes to elastin fragmentation in ascending aorta in MPS I mice. However, at 8 months, immunostaining of aorta with an anti-EBP antibody [9] that recognizes the mouse protein (A. Hinek, personal communication) was negative for both normal and MPS I mouse aortas (data not shown), which is consistent with the low EBP mRNA levels at this age (Fig. 2).

Our data strongly favor the hypothesis that elastin degradation was the major cause of the fragmented fibers in MPS I mice at late times. Since RNA for MMP-12 and cathepsin S were 23- and 11-fold normal, respectively, these elastin-degrading proteins might be responsible. Indeed, enzyme activity against an MMP-12 substrate was 8-fold normal in MPS I mice, although it remains possible that another metalloproteinase such as MMP-3 was responsible. In addition, cathepsin activity was 65-fold normal in MPS I mice with an assay that was performed at a neutral pH at which cathepsin S is active but most other cathepsins are inactive [20] and this activity was extremely sensitive to a cathepsin S-specific inhibitor. Although it is likely that each enzyme can act independently to cleave elastin, we plan to breed MPS I mice with MMP-12 [34] and/or cathepsin S [35] deficient mice to directly test the role of

each protein in the pathogenesis of disease in the aorta and other sites. Since both MMP-12 [25] and cathepsin S [36] are expressed by vascular smooth muscle cells (VSMC) *in vitro*, and there was no evidence of migration of macrophages into the aorta as assessed by immunostaining for Mac I (data not shown), VSMC were probably the source of MMP-12 and cathepsin S expression.

Role of STAT proteins in upregulation of MMP-12 and cathepsin S

We propose that activation of STAT-1 and/or STAT-3 in MPS I mice by phosphorylation resulted in upregulation of MMP-12 and cathepsin S. As noted above, the MMP-12 promoter has a sequence that is predicted to bind to STAT-1 and STAT-3. Although the cathepsin S promoter does not have a respectable STAT binding site, cathepsin S expression in VSMC was activated by IL-6 in a STAT-3-dependent process [37], which probably involved upregulation of IRF proteins. Indeed, mRNA for IRF-8 and IRF-3 were increased in the ascending aorta of MPS I mice, and these proteins may function in a similar fashion on the cathepsin S promoter as IRF-1 [27]. In addition, TIMP-1 is regulated by STAT-3 [38], and its mRNA was 4-fold normal (Fig. 2). It is interesting that mechanical stress to cultured VSMC resulted in phosphorylation of STAT-3 in a src-dependent fashion [39]. We propose that the stress on the cell from accumulation of lysosomal storage material may activate STAT-1 and STAT-3, although alternative explanations are possible.

Role of other transcription factors in upregulation of MMP-12 and cathepsin S

The MMP-12 promoter also contains a binding site for PEA3, which is activated by MAPK [40] and we showed here that MAPK was phosphorylated at sites that increase its activity. In addition, the osteopontin promoter contains a PEA3 binding site [41], and osteopontin mRNA was 16-fold normal in MPS I mice. PU.1 is an ets family transcription factor that acts synergistically with IRF-8 to induce expression of genes [42], and is expressed in VSMC [43] and regulates cathepsin S and osteopontin expression. PU.1 mRNA levels were 3-fold normal at 6 months in MPS I mice.

Implications of this study

This study suggests that up-regulation of MMP-12 and/or cathepsin S may be pivotal to the development of aortic dilatation and valvular degeneration in MPS I and related diseases. In addition, these proteins may contribute to manifestations of disease in other organs, such as skin, ligaments, and tendons. Indeed, MMPs contributed to joint disease in other MPS models [44] while cathepsin S was upregulated in the brain of MPS I mice [45]. If the genetic cross that is in progress shows that deficiency of one or both of these elastase proteins can reduce aortic disease in MPS I, it might be possible to treat MPS I patients with inhibitors of MMP-12 [46] and/or cathepsin S [47].

Sources of funding

This work was supported by the Ryan Foundation, the National MPS Society, and the National Institutes of Health (DK66448). Histology was supported by P30 DK52574 and real-time PCR was supported by DK20579 awarded to Clay Semenkovich.

Acknowledgments

We thank Alexander Hinek for the anti-EBP antibody, Xu Zhang for performing immunostaining, Elizabeth Neufeld for MPS I mice, Robert Thompson and John Curci for helpful discussions, and Clay Semenkovich and Trey Coleman for help with real-time PCR.

Appendix A. Supplementary data

Supplementary data associated with this article can be found, in the online version, at doi:10.1016/j.ymgme.2008.03.018.

References

[1] E.F. Neufeld, J. Muenzer, The mucopolysaccharidosis, in: C.R. Scriver, A.L. Beaudet, W.S. Sly, D. Valle (Eds.), Metabolic and Molecular Basis of Inherited Disease, McGraw Hill, New York, 2001, pp. 3421–3452.
[2] V.G. Renteria, V.J. Ferrans, W.C. Roberts, The heart in the hurler syndrome: gross, histologic and ultrastructural observations in five necropsy cases, Am. J. Cardiol. 38 (1976) 487–501.
[3] E. Braunlin, S. Mackey-Bojack, A. Panoskaltsis-Mortari, J.M. Berry, R.T. McElmurry, M. Riddle, L.-Y. Sun, L.A. Clarke, J. Tolar, B.R. Blazar, Cardiac functional and histopathologic findings in humans and mice with mucopolysaccharidosis type I: implications for assessment of therapeutic interventions in hurler syndrome, Pediatr. Res. 59 (2006) 27–32.
[4] R.E. Gompf, R.M. Shull, M.A. Breider, J.A. Scott, G.C. Constantopoulos, Cardiovascular changes after bone marrow transplantation in dogs with mucopolysaccharidosis I, Am. J. Vet. Res. 51 (1990) 2054–2060.
[5] A.M. Traas, P. Wang, X. Ma, M. Tittiger, L. Schaller, P. O'donnell, M.M. Sleeper, C. Vite, R. Herati, G.D. Aguirre, M. Haskins, K.P. Ponder KP, Correction of clinical manifestations of canine mucopolysaccharidosis I with neonatal retroviral vector gene therapy, Mol. Ther. 15 (2007) 1423–1431.
[6] M.D. Jordan, Y. Zheng, S. Ryazantsev, N. Rozengurt, K.P. Roos, E.F. Neufeld, Cardiac manifestations in the mouse model of mucopolysaccharidosis I, Mol. Genet. Metab. 86 (2005) 233–243.
[7] Y. Liu, L. Xu, A.K. Hennig, A. Kovacs, A. Fu, S. Chung, D. Lee, B. Wang, R.S. Herati, O.J. Mosinger, S.-R. Cai, K.P. Ponder, Liver-directed neonatal gene therapy prevents cardiac, bone, ear, and eye disease in mucopolysaccharidosis I mice, Mol. Ther. 11 (2005) 35–47.
[8] S.M. Mithieux, A.S. Weiss, Elastin, Adv. Protein Chem. 70 (2005) 437–461.
[9] A. Hinek, S.E. Wilson, Impaired elastogenesis in Hurler disease: dermatan sulfate accumulation linked to deficiency in elastin-binding protein and elastic fiber assembly, Am. J. Pathol. 156 (2000) 925–938.
[10] J.R. Barbour, F.G. Spinale, J.S. Ikonomidis, Proteinase systems and thoracic aortic aneurysm progression, J. Surg. Res. 139 (2007) 292–307.
[11] G.K. Sukhova, G.-P. Shi, Do cathepsins play a role in abdominal aortic aneurysm pathogenesis?, Ann NY Acad. Sci. 1085 (2006) 161–169.
[12] G.M. Longo, S.J. Buda, N. Fiotta, W.-F. Xiong, T. Griener, S. Shapiro, B.T. Baxter, MMP-12 has a role in abdominal aortic aneurysms in mice, Surgery 137 (2005) 457–462.
[13] R. Pyo, J.K. Lee, J.M. Shipley, J.A. Curci, D.-L. Mao, S.J. Ziporin, T.L. Ennis, S.D. Shapiro, R.M. Senior, R.W. Thompson, Targeted gene disruption of matrix metalloproteinase-9 (gelatinase B) suppresses development of experimental abdominal aortic aneurysms, J. Clin. Invest. 105 (2000) 1641–1649.
[14] A. Luttun, E. Lutgens, A. Manderveld, K. Maris, D. Collen, P. Carmeliet, L. Moons, Loss of matrix-9 or matrix metalloproteinase-12 protects apolipoprotein E-deficient mice against atherosclerotic media destruction but differentially affects plaque growth, Circulation 109 (2004) 1408–1414.
[15] V. Lesauskaite, M.C. Epistolato, M. Castagnini, S. Urbonavicius, P. Tanganelli, Expression of matrix metalloproteinases, their tissue inhibitors, and osteopontin in the wall of thoracic and abdominal aortas with dilatative pathology, Hum. Pathol. 37 (2006) 1076–1084.
[16] J.S. Ikonomidis, J.R. Barbour, Z. Amani, R.E. Stroud, A.R. Herron, D.M. McClister, S.E. Camens, M.L. Lindsey, R. Mukherjee, F.G. Spinale, Effects of deletion of the matrix metalloproteinase 9 gene on development of murine thoracic aortic aneurysms, Circulation 112 (2005) I242–I248.
[17] K.U. Ogbureke, L.W. Fisher, Renal expression of SIBLING proteins and their partner matrix metalloproteinases (MMPs), Kidney Int. 68 (2005) 155–166.
[18] E. Allaire, R. Forough, M. Clowes, B. Starcher, A.W. Clowes, Local overexpression of TIMP-1 prevents aortic aneurysm degeneration and rupture in a rat model, J. Clin. Invest. 102 (1998) 1413–1420.
[19] W.-F. Xiong, R. Knispel, J. Mactaggart, B.T. Baxter, Effects of tissue inhibitor of metalloproteinase 2 deficiency on aneurysm formation, J. Vasc. Surg. 44 (2006) 1061–1066.
[20] D. Bromme, P.R. Bonneau, P. Lachance, B. Wiederanders, H. Kirschke, C. Peters, D.Y. Thomas, A.C. Storer, R. Vernet, Functional expression of human cathepsin S in *Saccharomyces cerevisiae*, J. Biol. Chem. 268 (1993) 4832–4838.
[21] E. Lutgens, B. Faber, K. Schapira, C.T. Evelo, R. van Haaften, S. Heeneman, K.B. Cleutjens, A.P. Bijnens, L. Beckers, J.G. Porter, C.R. Mackay, P. Rennert, V. Bailly, M. Jarpe, B. Dolinski, V. Koteliansky, T. de Fougerolles, M.J. Daemen, Gene profiling in atherosclerosis reveals a key role for small inducible cytokines: validation using a novel monocyte chemoattractant protein monoclonal antibody, Circulation 111 (2005) 3443–3452.
[22] G.K. Sukhova, Y.-O. Zhang, J.-H. Pan, Y. Wada, T. Yamamoto, M. Naito, T. Kodama, S. Tsimikas, J.L. Witztum, M.L. Lu, Y. Sakara, M.T. Chin, P. Libby, G.-P. Shi, Deficiency of cathepsin S reduces atherosclerosis in LDL receptor-deficient mice, J. Clin. Invest. 111 (2003) 897–906.

[23] J.E. Wagenseil, N.L. Nerurkar, R.H. Knutsen, R.J. Okamoto, D.Y. Li, R.P. Mecham, Effects of elastin haploinsufficiency on the mechanical behavior of mouse arteries, Am. J. Physiol. Heart Circ. Physiol. 289 (2005) H1209–H1217.
[24] B. Werle, A. Staib, B. Julke, W. Ebert, P. Zladoidsky, A. Sekirnik, J. Kos, E. Spiess, Fluorometric microassays for the determination of cathepsin L and cathepsin S activities in tissue extracts, Biol. Chem. 380 (1999) 1109–1116.
[25] L. Wu, A. Tanimoto, Y. Murata, T. Sasaguri, J. Fan, Y. Sasaguri, T. Watanabe, Matrix metalloproteinase-12 gene expression in human vascular smooth muscle cells, Genes Cells 8 (2003) 225–234.
[26] G.B. Ehret, P. Reichenbach, U. Schindler, C.M. Horvath, S. Fritz, M. Nabholz, P. Bucher, DNA binding specificity of different STAT proteins. Comparison of in vitro specificity with natural target sites, J. Biol. Chem. 276 (2001) 6675–6688.
[27] K. Honda, T. Taniguchi, IRFs: master regulators of signalling by toll-like receptors and cytosolic pattern-recognition receptors, Nat. Rev. Immunol. 6 (2006) 644–658.
[28] Y. Wang, R.M. Baron, G.-L. Zhu, M. Joo, J.W. Christman, E.S. Silverman, M.A. Perrella, R.J. Riese, M. Cernadas, PU.1 regulates cathepsin S expression in professional APCs, J. Immunol. 176 (2006) 275–283.
[29] J.P. Habashi, D.P. Judge, T.M. Holm, R.D. Cohn, B.L. Loeys, T.K. Cooper, L. Myers, E.C. Klein, G. Liu, C. Calvi, M. Podowski, E.R. Neptune, M.K. Halushka, D. Bedja, K. Gabrielson, D.B. Rifkin, L. Carta, F. Ramirez, D.L. Huso, H.C. Dietz, Losartan, an AT1 antagonist, prevents aortic aneurysm in a mouse model of Marfan syndrome, Science 312 (2006) 117–121.
[30] E.A. Braunlin, N.R. Stauffer, C.H. Peters, J.L. Bass, J.M. Berry, J.J. Hopwood, W. Krivit, Usefulness of bone marrow transplantation in the Hurler syndrome, Am. J. Cardiol. 92 (2003) 882–886.
[31] E.A. Braunlin, J.M. Berry, C.B. Whitley, Cardiac findings after enzyme replacement therapy for mucopolysaccharidosis type I, Am. J. Cardiol. 98 (2006) 416–418.
[32] M. Sifuentes, R. Doroshow, R. Hoft, G. Mason, I. Walot, M. Diament, S. Okazaki, K. Huff, G.F. Cox, S.J. Swiedler, E.D. Kakkis, A follow-up study of MPS I patients treated with laronidase enzyme replacement therapy for 6 years, Mol. Genet. Metab. 90 (2007) 171–180.
[33] H. Morreau, N.J. Galjart, N. Gillemans, R. Willemsen, G.T. van der Horst, A. d'Azzo, Alternative splicing of B-galactosidase mRNA generates the classic lysosomal enzyme and a B-galactosidase-related protein, J. Biol. Chem. 264 (1989) 20655–20663.
[34] J.M. Shipley, R.L. Wesselschmidt, D.K. Kobayashi, T.J. Ley, S.D. Shapiro, Metalloelastase is required for macrophage-mediated proteolysis and matrix invasion in mice, Proc. Natl. Acad. Sci. USA 93 (1996) 3942–3946.
[35] T.Y. Nakagawa, W.H. Brissette, P.D. Lira, R.J. Griffiths, N. Petrushova, J. Stock, J.D. McNeish, S.E. Eastman, E.D. Howard, S.R. Clarke, E.F. Rosloniec, E.A. Elliott, A.Y. Rudensky, Impaired invariant chain degradation and antigen presentation and diminished collagen-induced arthritis in cathepsin S null mice, Immunity 10 (1999) 207–217.
[36] G.K. Sukhova, G.P. Shi, D.I. Simon, H.A. Chapman, P. Libby, Expression of the elastolytic cathepsins S and K in human atheroma and regulation of their production in smooth muscle cells, J. Clin. Invest. 102 (1998) 576–583.
[37] H. Kitamura, H. Kamon, S. Sawa, S.J. Park, N. Katunuma, K. Ishihara, M. Murakami, T. Hirano, IL-6-STAT3 controls intracellular MHC class II alphabeta dimer level through cathepsin S activity in dendritic cells, Immunity 23 (2005) 491–502.
[38] J. Dien, H.M. Amin, N. Chiu, W. Wong, C. Frantz, B. Chiu, J.R. Mackey, R. Lai, Signal transducers and activators of transcription-3 up-regulates tissue inhibitor of metalloproteinase-1 expression and decreases invasiveness of breast cancer, Am. J. Pathol. 169 (2006) 633–642.
[39] J.D. Kakisis, S. Pradhan, A. Cordova, C.D. Liapis, B.E. Sumpio, The role of STAT-3 in the mediation of smooth muscle cell response to cyclic strain, Int. J. Biochem. Cell Biol. 37 (2005) 1396–1406.
[40] Y. de Launoit, J.L. Baert, A. Chotteau-Lelievre, D. Monte, L. Coutte, S. Mauen, V. Firlej, C. Degerny, K. Verreman, The Ets transcription factors of the PEA3 group: transcriptional regulators in metastasis, Biochim. Biophys. Acta 1766 (2006) 79–87.
[41] S. Fujihara, M. Yokozeki, Y. Oba, Y. Higashibata, S. Nomura, K. Moriyama, Function and regulation of osteopontin in response to mechanical stress, J. Bone Miner. Res. 21 (2006) 956–964.
[42] T. Tamura, K. Ozato, ICSBP/IRF-8: its regulatory roles in the development of myeloid cells, J. Interferon Cytokine Res. 22 (2002) 145–152.
[43] T. Inaba, T. Gotoda, S. Ishibashi, K. Harada, J.I. Ohsuga, K. Ohashi, Y. Yazaki, N. Yamada, Transcription factor PU.1 mediates induction of c-fms in vascular smooth muscle cells: a mechanism for phenotypic change to phagocytic cells, Mol. Cell. Biol. 16 (1996) 2264–2273.
[44] C.M. Simonaro, M. D'Angelo, M.E. Haskins, E.H. Schuchman, Joint and bone disease in mucopolysaccharidosis VI and VII: identification of new therapeutic targets and biomarkers using animal models, Pediatr. Res. 57 (2005) 701–707.
[45] K. Ohmi, D.S. Greenberg, K.S. Rajavel, S. Ryazantsev, H.H. Li, E.F. Neufeld, Activated microglia in cortex of mouse models of mucopolysaccharidosis I and IIIB, Proc. Natl. Acad. Sci. USA 100 (2003) 1902–1907.
[46] L. Devel, V. Rogakos, A. David, A. Makaritis, F. Beau, P. Cuniasse, A. Yiotakis, V. Dive, Development of selective inhibitors and substrate of matrix metalloproteinase-12, J. Biol. Chem. 281 (2006) 11152–11160.
[47] J.O. Link, S. Zipfel, Advances in cathepsin S inhibitor design, Curr. Opin. Drug Discov. Dev. 9 (2006) 471–482.